

Cosmic Microwave Background map-making solutions improve with cooling

BAI-QIANG QIANG (KMH: WANT CHINESE CHARACTERS?)¹ AND KEVIN M. HUFFENBERGER ¹

¹*Department of Physics, Florida State University, Tallahassee, Florida 32306*

ABSTRACT

In the context of Cosmic Microwave Background data analysis, we study the solution to the equation that transforms scanning data into a map. As originally suggested in “messenger” methods for solving linear systems, we split the noise covariance into uniform and non-uniform parts and adjusting their relative weight during the iterative solution. This “cooling” or perturbative approach is particularly effective when there is significant low-frequency noise in the timestream. A conjugate gradient algorithm applied to this modified system converges faster and to a higher fidelity solution than the standard conjugate gradient approach, for the same computational cost per iteration. We conclude that cooling is helpful separate from its appearance in the messenger methods. We give an analytical expression for the parameter that controls how gradually should change during the course of the solution.

Keywords: Computational methods — Cosmic microwave background radiation — Astronomy data reduction

1. INTRODUCTION

In observations of the Cosmic Microwave Background (CMB), map-making is an intermediate step between the collection of raw scanning data and the scientific analyses, such as the estimation of power spectra and cosmological parameters. Next generation CMB observations will generate much more data than today, and so it is worth exploring efficient ways to process the data, even though, on paper, the map-making problem has long been solved.

The time-ordered scanning data is summarized by

$$\mathbf{d} = P\mathbf{m} + \mathbf{n} \quad (1)$$

where \mathbf{d} , \mathbf{m} , and \mathbf{n} are the vectors of time-ordered data (TOD), the CMB sky-map signal, and measurement noise, and P is the sparse matrix that encodes the telescope’s pointing. Of several mapmaking methods (Tegmark 1997), one of the most common is the method introduced for the Cosmic Background Explorer (COBE, Janssen & Gulkis 1992). This optimal, linear solution is

$$(P^\dagger N^{-1} P)\hat{\mathbf{m}} = P^\dagger N^{-1} \mathbf{d} \quad (2)$$

where $\hat{\mathbf{m}}$ provides the generalized least squares minimization of the χ^2 statistic

$$\chi^2(\mathbf{m}) \equiv (\mathbf{d} - P\mathbf{m})^\dagger N^{-1} (\mathbf{d} - P\mathbf{m}). \quad (3)$$

Here we assume that the noise has zero mean $\langle \mathbf{n} \rangle = \mathbf{0}$, and noise covariance matrix could be written as $N = \langle \mathbf{nn}^\dagger \rangle$. We cast mapmaking as a standard linear regression problem. In case the noise is Gaussian, the COBE solution is also the maximum likelihood solution.

With current computation power, we cannot solve for $\hat{\mathbf{m}}$ by calculating $(P^\dagger N^{-1} P)^{-1} P^\dagger N^{-1} \mathbf{d}$ directly, since the $(P^\dagger N^{-1} P)$ matrix is too large to invert. The noise covariance matrix N is sparse in frequency domain and the pointing matrix P is sparse in the time-by-pixel domain, and their product is dense. In experiments currently under design, there may be $\sim 10^{16}$ time samples and $\sim 10^9$ pixels, so these matrix inversions are intractable. Therefore we use iterative methods, such as conjugate gradient descent, to avoid the matrix inversions, while executing each matrix multiplication in a basis where the matrix is sparse, using a fast Fourier transform to go between the frequency and time domain.

As an alternative technique, Huppenberger & Naess (2018) showed that the “messenger method” could be adapted to solve the linear mapmaking system, based on the approach from Elsner & Wandelt (2013) to solve the linear Wiener filter. This technique splits the noise covariance into a uniform part and the remainder, and, over the course of the iterative solution, it adjusts the relative weight of those two parts. Starting with the uniform covariance, the modified linear system gradually transforms to the final system via a cooling parameter. The cooling idea again comes from Elsner & Wan-

delt (2013). In numerical experiments, Huffenberger & Næss (2018) found that the large scales of map produced by the cooled messenger method converged significantly faster than for standard methods, and to higher fidelity.

Papež et al. (2018) showed that the iterations in the messenger field approach is equivalent to a fixed point iteration scheme, and studied its convergence properties in detail. Furthermore, they showed that the split covariance and the modified system that incorporates the cooling can be solved by other means, including a conjugate gradient technique, which should generally show better convergence properties than the fixed-point scheme. However in numerical tests, Papež et al. (2018) did not find benefits to the cooling modification of the mapmaking system, in contrast to findings of Huffenberger & Næss (2018).

In this paper, we show that the difference arose because the numerical tests in Papež et al. (2018) used much less low-frequency ($1/f$) noise than Huffenberger & Næss (2018), and show that the cooling technique improves mapmaking performance especially when the low frequency noise is large. This performance boost depends on a proper choice for the pace of cooling. Kodi Ramanah et al. (2017) showed that for Wiener filter the cooling parameter should be chosen as a geometric series. In this work, we give an alternative interpretation of the parameterizing process and show that for mapmaking the optimal choice (unsurprisingly) is also a geometric series.

In Section 2 we describe our methods for treating the mapmaking equation and our numerical experiments. In Section 3 we present our results. In Section 4 we interpret the mapmaking approach and its computational cost. In Section 5 we conclude. In appendices we derive how we set our cooling schedule.

2. METHODS

2.1. Parameterized Conjugate Gradient Method

The messenger field approach introduced an extra cooling parameter λ to the map-making equation, and solved the linear system with the alternative covariance $N(\lambda) = \lambda\tau I + \bar{N}$. The parameter τ represents the uniform level of (white) noise in the covariance, \bar{N} is the balance of the noise, and the parameterized covariance equals the original covariance when the cooling parameter $\lambda = 1$. In this work we find it more convenient to work with the inverse cooling parameter $\eta = \lambda^{-1}$ and define the covariance as

$$N(\eta) = \tau I + \eta \bar{N} \quad (4)$$

which leads to the same system of mapmaking equations. (This is because $N(\eta) = \lambda^{-1}N(\lambda)$ and the mapmaking

equation is insensitive to scalar multiple of the covariance since it appears on both sides.)

Papež et al. (2018) showed that the conjugate gradient method can be easily applied to parameterized mapmaking equation by iterating on

$$P^\dagger N(\eta)^{-1} P \hat{\mathbf{m}} = P^\dagger N(\eta)^{-1} \mathbf{d} \quad (5)$$

as the cooling is adjusted. In our numerical experiments, we confirm that the conjugate gradient approach is converging faster than the fixed point iterations suggested by the messenger mapmaking method in Huffenberger & Næss (2018). For simplicity we fix the preconditioner to $M = P^\dagger P$ for all of calculations.

When $\eta = 0$, the noise covariance matrix $N(0)$ is proportional to identity matrix I , and solution is given by simple binned map $\mathbf{m}_0 = (P^\dagger P)^{-1} P^\dagger \mathbf{d}$, which can be solved directly. From this starting point, the cooling scheme requires the inverse cooling parameter η increase as $0 = \eta_0 \leq \eta_1 \leq \dots \leq \eta_{\text{final}} = 1$, at which point we arrive at the desired mapmaking equation. For each intermediate η_i , we treat it as a separate conjugate gradient method to solve equation $(P^\dagger N(\eta_i)^{-1} P) \hat{\mathbf{m}}(\eta_i) = P^\dagger N(\eta_i)^{-1} \mathbf{d}$, using the result from previous calculation $\hat{\mathbf{m}}(\eta_{i-1})$ as the initial value, and move to next parameter η_{i+1} when $(P^\dagger N(\eta_i)^{-1} P) \hat{\mathbf{m}}(\eta_i) - P^\dagger N(\eta_i)^{-1} \mathbf{d} \simeq 0$. KMH: In this description, it is not totally clear whether you intend to update the eta after every iteration.

The non-white part \bar{N} is the troublesome portion of the covariance, and we can think of the η parameter as turning it on slowly, adding a perturbation to the solution achieved at a particular stage, building ultimately upon the initial uniform covariance model.

2.2. Choice of inverse cooling parameters η

The next question is how we choose these monotonically increasing parameters η . If we choose them inappropriately, the solution converge slowly, because we waste effort converging on the wrong system. We also want to determine $\eta_1, \dots, \eta_{n-1}$ before starting conjugate gradient iterations. The time ordered data \mathbf{d} is very large, and we do not want to keep it in the system memory during calculation. If we determine $\eta_1, \dots, \eta_{n-1}$ before the iterations, then we can precompute the right-hand side $P^\dagger N(\eta)^{-1} \mathbf{d}$ for each η_i and keep these map-sized objects in memory, instead of the entire time-ordered data.

In the appendix, we show that a generic good choice for the η parameters are the geometric series

$$\eta_i = \min \left\{ (2^i - 1) \frac{\tau}{\max(\bar{N}_f)}, 1 \right\}, \quad (6)$$

where \bar{N}_f is the frequency representation of the non-uniform part of the covariance. This is the main result.

It tells us not only how to choose parameters η_i , but also when we should stop the perturbation, and set $\eta = 1$. For example, if noise covariance matrix N is almost white noise, then $\bar{N} = N - \tau I \approx 0$, and we would have $\tau/\max(\bar{N}_f) \gg 1$. This tell us that we don't need to use parameterized method at all, because $\eta_0 = 0$ and $\eta_1 = \eta_2 = \dots = 1$. This corresponds to the standard conjugate gradient method with simple binned map as the initial guess (as recommended by Papež et al. 2018).

2.3. Numerical Simulations

To compare these algorithms, we need to do some simple simulation of scanning processes, and generate time ordered data from random sky signal.¹ Our sky is a small rectangular area, with two orthogonal directions x and y , both with range from -1° to $+1^\circ$. The signal has first three stokes parameters (I, Q, U).

For the scanning process, our single telescope contains nine detectors, each has different sensitivity to polarization Q and U . It scans the sky with a raster scanning pattern and scanning frequency $f_{\text{scan}} = 0.1$ Hz sampling frequency $f_{\text{sample}} = 100$ Hz. The telescope scans the sky horizontally and then vertically, and then digitizes the position (x, y) into 512×512 pixel. This gives noiseless signal \mathbf{s} .

The noise power spectrum is given by

$$P(f) = \sigma^2 \left(1 + \frac{f_{\text{knee}}^\alpha + f_{\text{apo}}^\alpha}{f^\alpha + f_{\text{apo}}^\alpha} \right) \quad (7)$$

Here we fixed $\sigma^2 = 10 \mu\text{K}^2$, $\alpha = 3$, and $f_{\text{knee}} = 10$ Hz, and change f_{apo} to compare the performance under different noise models. Dünner et al. (2013) measured the slopes of the atmospheric noise in the Atacama under different water vapor conditions, finding $\alpha = 2.7$ to 2.9 . Note that as $f_{\text{apo}} \rightarrow 0$, $P(f) \rightarrow \sigma^2(1 + (f/f_{\text{knee}})^{-\alpha})$, it becomes a $1/f$ noise model. The noise covariance matrix

$$N_{ff'} = P(f) \frac{\delta_{ff'}}{\Delta_f} \quad (8)$$

is a diagonal matrix in frequency space, where Δ_f is equal to reciprocal of total scanning time $T \approx 1.05 \times 10^4$ seconds. In our calculations we choose different combination of f_{knee} and f_{apo} , some of the power spectrum are shown in Figure(1).

Finally, we get the simulated time ordered data $\mathbf{d} = \mathbf{s} + \mathbf{n}$ by adding up signal and noise.

3. RESULTS

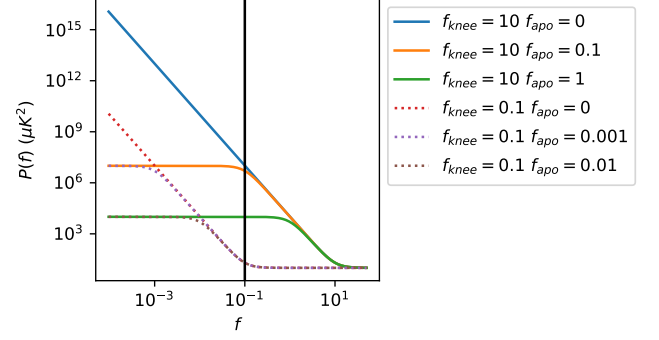


Figure 1. The noise power spectrum based on Eq. (7) with $\sigma^2 = 10 \mu\text{K}^2$ and $\alpha = 3$. Two knee frequencies $f_{\text{knee}} = 10$ (solid lines) and $f_{\text{knee}} = 0.1$ (dashed lines). For each knee frequency, we have $f_{\text{apo}} = 0, 0.1f_{\text{knee}}$ and $0.01f_{\text{knee}}$. The vertical line shows our scanning frequency.

First let's compare the results with vanilla conjugate gradient method with simple preconditioner $P^\dagger P$. Figure (2) shows the results for $1/f$ noise model ($f_{\text{apo}} = 0$) with different knee frequency. In Figure (3) we fixed $f_{\text{knee}} = 10$ Hz, and change f_{apo} . Here note that χ^2 in all figures are calculated based on Eq. (3) not $\chi^2(\mathbf{m}, \eta)$ in Eq. (A1). The χ^2_{min} is calculated from perturbative conjugate gradient method with 100 η values, and it stops when the norm of residual $\|\mathbf{r}\| = \|P^\dagger N^{-1} \mathbf{d} - (P^\dagger N^{-1} P) \mathbf{m}\|$ per pixel is smaller than 10^{-10} , or after 1000 iterations.

As we can see in Figure (2) and the first graph in Figure (3), for $1/f$ noise model, when $f_{\text{knee}} \gtrsim 10f_{\text{scan}}$ the parameterized method starts showing advantage over vanilla conjugate gradient method. From Figure (3) we can see that as we increase f_{apo} while fix f_{knee} , these two methods performs similar.

If we look at the power spectrum in Figure (1), when f_{knee} is small or f_{apo} is large there are not many large scale low frequency noise. So introducing η parameter could improve perform when there are large low noise contribution.

We also tried different α values. For $\alpha = 2$, the conclusion is the same as $\alpha = 3$. When $\alpha = 1$, there are not many low frequency noise, the vanilla conjugate gradient is preferred, except some cases with very large knee frequency like $f_{\text{knee}} = 100$ Hz and $f_{\text{apo}} = 0$ would favour parameterized method. In Papež et al. 2018, the $\alpha = 1$ and the noise power spectrum is apodized at $0.1f_{\text{knee}}$, which corresponds to $f_{\text{apo}} \approx 0.1f_{\text{knee}}$, and their knee frequency is the same as scanning frequency, so $f_{\text{knee}} = f_{\text{scan}} = 0.1$ in our cases. In their case there are not many low frequency noise, and we confirm that vanilla conjugate gradient method would converge faster.

¹ The source code and other information are available at https://github.com/Bai-Qiang/map_making_perturbative_approach

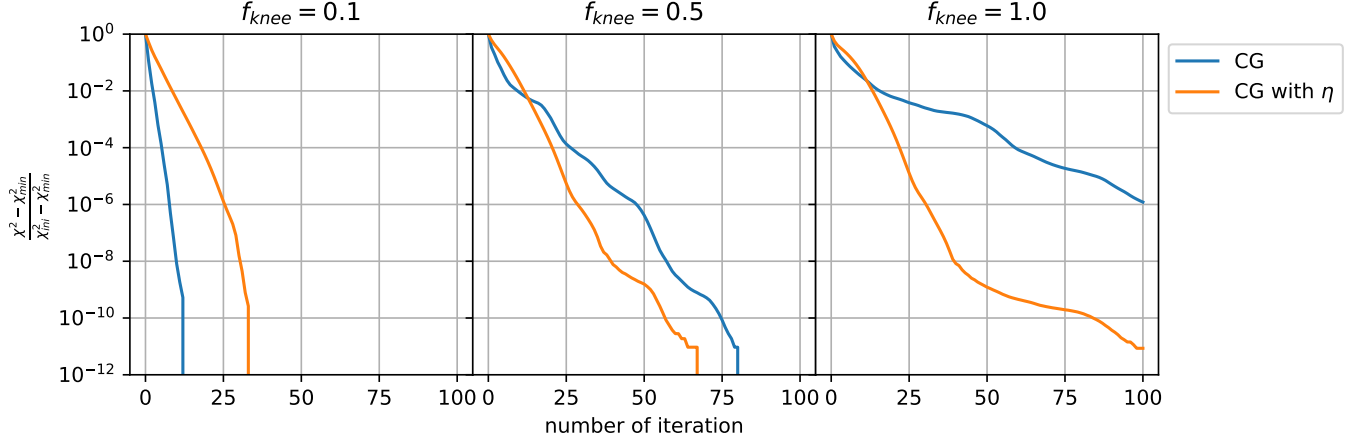


Figure 2. These three figures show the $\frac{\chi^2(\mathbf{m}) - \chi^2_{\min}}{\chi^2_{\text{ini}} - \chi^2_{\min}}$ changes for each iteration under different noise covariance matrix with fixed $f_{\text{apo}} = 0$ and f_{knee} being 0.1, 0.5, and 1.0.

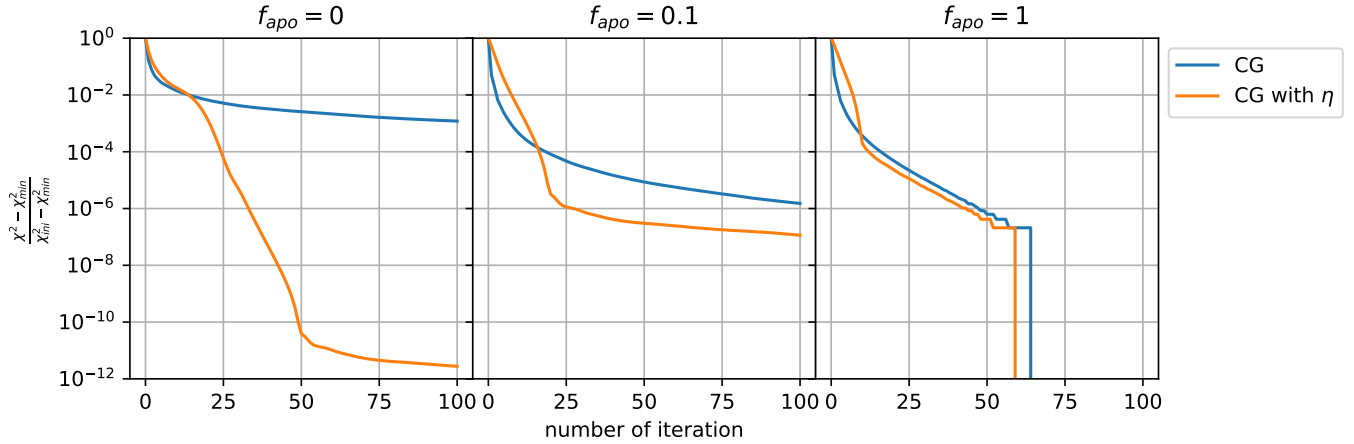


Figure 3. These three figures show the $\frac{\chi^2(\mathbf{m}) - \chi^2_{\min}}{\chi^2_{\text{ini}} - \chi^2_{\min}}$ changes for each iteration under different noise covariance matrix with fixed $f_{\text{knee}} = 10$ and f_{apo} being 0, 0.1, and 1.0.

4. DISCUSSION

4.1. Intuitive Interpretation of η

KMH: most of this is pretty similar to discussion in Huffenberger and Naess. The last paragraph is new.

In this section, let me introduce another way to understand the role of η . Our ultimate goal is to find $\hat{\mathbf{m}}(\eta = 1)$ which minimizes $\chi^2(\mathbf{m}) = (\mathbf{d} - \mathbf{P}\mathbf{m})^\dagger N^{-1}(\mathbf{d} - \mathbf{P}\mathbf{m})$. Since N is diagonal in frequency space, χ^2 could be written as a sum of all frequency mode $|(\mathbf{d} - \mathbf{P}\mathbf{m})_f|^2$ with weight N_f^{-1} , such as $\chi^2(\mathbf{m}) = \sum_f |(\mathbf{d} - \mathbf{P}\mathbf{m})_f|^2 N_f^{-1}$. N_f^{-1} is large when there is little noise at that frequency, and vice versa. Which means $\chi^2(\mathbf{m})$ would favor the low noise frequency mode over high noise ones. In other words the optimal map $\hat{\mathbf{m}}$ focusing on minimize the error $\mathbf{r} \equiv \mathbf{d} - \mathbf{P}\mathbf{m}$ in the low-noise part.

After introducing η , we minimize $\chi^2(\mathbf{m}, \eta) = (\mathbf{d} - \mathbf{P}\mathbf{m})^\dagger N_{\eta=0}^{-1}(\mathbf{d} - \mathbf{P}\mathbf{m})$. For $\eta = 0$, $N_{\eta=0}^{-1} \propto I$ and the esti-

mated map $\hat{\mathbf{m}}(\eta = 0)$ does not prioritize any frequency mode. As we slowly increase η , we decrease the weight for the frequency modes which have large noise, and focusing minimizing error for low noise part. If we start with $\eta_1 = 1$ directly, which corresponds to the vanilla conjugate gradient method, then the entire conjugate gradient solver will focus most on minimizing the low noise part, such that χ^2 would converge very fast at low noise region, but slowly on high noise part. Since it focus on low noise part only, it may be stuck at some local minimum point. To get to the global minimum, it need to adjust the low noise part, that would be difficult if it's stuck at a local minimum. However by introducing η parameter, we let the solver first treat every frequency equally. Then as η slowly increases, it gradually shifts focus from the highest noise to the lowest noise part.

284 **KMH: I feel what this is missing is why the high-noise**
 285 **modes get stuck though.**

286 If we write the difference between final and
 287 initial χ^2 value as $\chi^2(\hat{\mathbf{m}}(1), 1) - \chi^2(\hat{\mathbf{m}}(0), 0) =$
 288 $\int_0^1 d\eta \frac{d}{d\eta} \chi^2(\hat{\mathbf{m}}(\eta), \eta)$, and use Eq. (A2). We note that
 289 when η is very small, the $\frac{d}{d\eta} \chi^2(\hat{\mathbf{m}}(\eta), \eta)$ would have rel-
 290 atively large contribution from medium to large noise
 291 region, comparing to large η . So introducing η might
 292 improve the convergence of χ^2 at these regions, because
 293 the vanilla conjugate gradient method only focuses on
 294 the low noise part and it may have difficulty at these
 295 regions.

4.2. Computational Cost

297 To properly compare the performance cost of this
 298 method with respect to vanilla conjugate gradient
 299 method with simple preconditioner, we need to com-
 300 pare their computational cost at each iteration. The
 301 right hand side of parameterized map-making equation
 302 Eq. (5) could be computed before iterations, so it won't
 303 introduce extra computational cost. The most demand-
 304 ing part of conjugate gradient method is calculating
 305 $P^\dagger N^{-1} P \hat{\mathbf{m}}$, because it contains a Fourier transform of
 306 $P \hat{\mathbf{m}}$ from time domain to frequency domain and an in-
 307 verse Fourier transform of $N^{-1} P \hat{\mathbf{m}}$ from frequency do-
 308 main back to time domain, which is order $\mathcal{O}(n \log n)$
 309 with n being the length of time ordered data. If we
 310 change N^{-1} to $N(\eta)^{-1}$, it won't add extra cost, since
 311 both matrices are diagonal in frequency domain. There-
 312 fore the computational cost it the same for one step.

313 However our previous analysis is based on
 314 $\chi^2(\hat{\mathbf{m}}(\eta_i), \eta_i)$ which is evaluated at $\hat{\mathbf{m}}(\eta_i)$ the esti-
 315 mated map at η_i . So We should update η_i to η_{i+1}
 316 when $\mathbf{m} \approx \hat{\mathbf{m}}(\eta_i)$. How do we know this condition is
 317 satisfied? Since for each new η_i value, we are solving
 318 a new set of linear equations $A(\eta_i) \hat{\mathbf{m}} = \mathbf{b}(\eta_i)$ with
 319 $A(\eta_i) = P^\dagger N(\eta_i)^{-1} P$ and $\mathbf{b}(\eta_i) = P^\dagger N(\eta_i)^{-1} \mathbf{d}$, and we
 320 could stop calculation and moving to next value η_{i+1}
 321 when the norm of residual $\|\mathbf{r}(\eta_i)\| = \|\mathbf{b}(\eta_i) - A(\eta_i) \hat{\mathbf{m}}\|$
 322 smaller than some small value. Calculate $\|\mathbf{r}(\eta_i)\|$ is
 323 part of conjugate gradient algorithm, so this won't
 324 add extra cost compare to vanilla conjugate gradient
 325 method. Therefore, overall introducing η won't have
 326 extra computational cost.

4.3. Other η Choises

327
 328 Now let us compare the performance difference
 329 between choosing η parameters based on Eq. (6)
 330 and manually fixing number of η parameters n_η
 331 manually. We manually choose the η_i values us-
 332 ing function `numpy.logspace(start=ln(η_1), stop=0,`
 333 `num= n_η , base= e)`. The results are showed in Figure (4).

334 Since the η values determined from Eq. (6)

$$335 \quad \eta_i = \min \left\{ 1, \frac{\tau}{\max(N_f)} (2^i - 1) \right\} \quad (6)$$

336
 337 are not dependent on any scanning information, it only
 338 depends on noise power spectrum $P(f)$, or noise covari-
 339 ance matrix N . Figure (??) and Figure (??) show two
 340 examples with same parameters as in Figure (??) except
 341 for the scanning frequency f_{scan} in Figure (??) it scans
 342 very slow and in Figure (??) it's very fast. In these
 343 two cases under $1/f$ noise model, our η values based on
 344 Eq. (6) are better than manually selected values. Based
 345 on these two results we know, the η values should some-
 346 how depends on scanning scheme.

4.4. Future Prospects

347
 348 **KMH: some of this future prospects should move to**
 349 **discussion** As you may have noticed in the second and
 350 third Figure(??), the perturbation parameter based on
 351 Eq. (6) is more than needed, especially for $1/f$ noise
 352 case. For the case $\kappa = 10^{12}$, we notice that based on
 353 Eq. (6) it gives us $n_\eta \approx 40$, however from χ^2 result in the
 354 last Figure(??) $n_\eta \approx 30$ or even $n_\eta \approx 15$ is good enough.
 355 Also, for the nearly-white-noise case, we could certainly
 356 choose $n_\eta = 1$ such that $\eta_1 = 1$ which corresponds to
 357 vanilla conjugate gradient method, based on χ^2 result
 358 in first Figure(??). However Eq. (6) gives us $n_\eta \approx 6$,
 359 even though it does not make the final χ^2 result much
 360 different at the end.

361 Is it possible to further improve the analysis, such that
 362 it produces smaller n_η ? Let's examine how we get η_i
 363 series. Remember that we determine $\delta\eta$ value based
 364 on the upper bound of $-\delta\chi^2(\hat{\mathbf{m}}(\eta), \eta)/\chi^2(\hat{\mathbf{m}}(\eta), \eta)$, in
 365 Eq. (??). For $\eta \neq 0$, the upper bound is

$$366 \quad \delta\eta \frac{\hat{\mathbf{r}}_\eta^\dagger N(\eta)^{-1} \bar{N} N(\eta)^{-1} \hat{\mathbf{r}}_\eta}{\hat{\mathbf{r}}_\eta^\dagger N(\eta)^{-1} \hat{\mathbf{r}}_\eta} \leq \frac{\delta\eta}{\eta + \frac{\tau}{\max(N_f) - \tau}} \quad (9)$$

367
 368 with $\mathbf{r}_\eta = \left[1 - P(P^\dagger N(\eta)^{-1} P)^{-1} P^\dagger N(\eta)^{-1} \right] \mathbf{d} \equiv \mathcal{P}_\eta \mathbf{d}$.
 369 To get the upper bound we treated $\mathbf{d} - P \hat{\mathbf{m}}(\eta)$ as an ar-
 370 bitrary vector in frequency domain, since we don't know
 371 how to calculate \mathcal{P}_η for $\eta \neq 0$, and it's hard to analyze
 372 the projection matrix \mathcal{P}_η in frequency space, as it con-
 373 tains $(P^\dagger N(\eta)^{-1} P)^{-1}$. Note that we have to determine
 374 all of η value before calculation, because we don't want
 375 to keep the time ordered data in system RAM, so we
 376 need to somehow analytically analyze \mathcal{P}_η , and its be-
 377 havior in frequency space. Unless \mathbf{r}_η almost only has
 378 large noise modes, $\left| \frac{d}{d\eta} \chi^2(\hat{\mathbf{m}}(\eta), \eta) / \chi^2(\hat{\mathbf{m}}(\eta), \eta) \right|$ won't
 379 get close to the upper bound $1/\left(\eta + \frac{\tau}{\max(N_f) - \tau}\right)$. Based

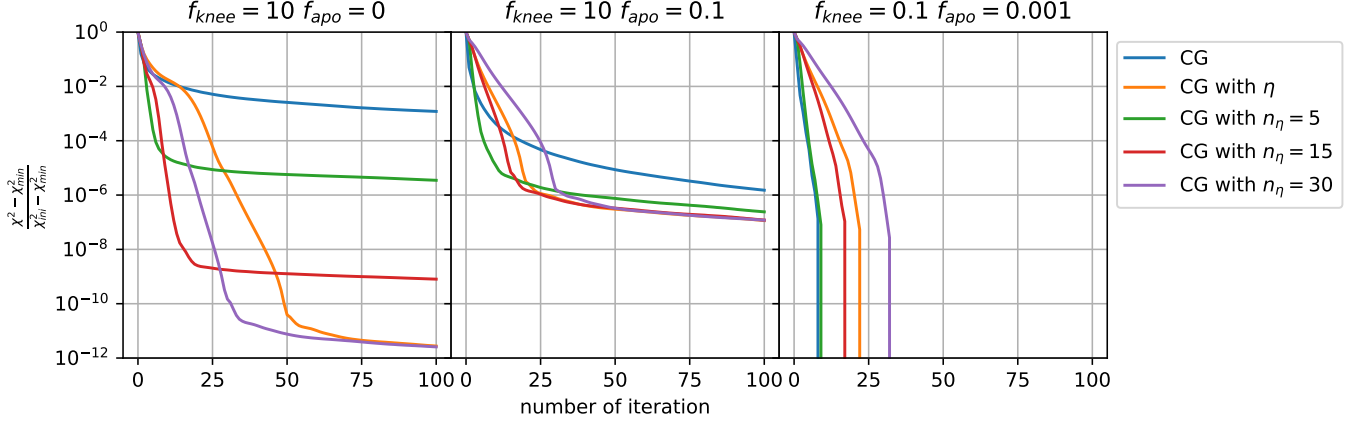


Figure 4. The blue line and the orange line are vanilla conjugate gradient method and parameterized conjugate gradient method. For three extra lines, we fix the number of η parameter n_η manually. Instead of using Eq. (6), we use `numpy.logspace(start=ln(η_1), stop=0, num= n_η , base=e)` to get all η parameters.

on the analysis in Section(4.1), for small η the estimated map $\hat{\mathbf{m}}(\eta)$ does not only focusing on minimizing error \mathbf{r}_η at low noise region. So we would expect that there would be a fair amount of low noise modes contribution in \mathbf{r}_η especially for the first few η values. Which means if we could somehow know the frequency distribution of \mathbf{r}_η , we could tighten the boundary of $\left| \frac{d}{d\eta} \chi^2(\hat{\mathbf{m}}(\eta), \eta) / \chi^2(\hat{\mathbf{m}}(\eta), \eta) \right|$, and get larger $\delta\eta$ value. This should make η goes to 1 faster, and yields the fewer η parameters we need.

Also notice that the η values determined from Eq. (6) are not dependent on any scanning information, it only depends on noise power spectrum $P(f)$, or noise covariance matrix N . In Appendix ?? we would show two examples with same parameters as in Figure(??) except scanning frequency f_{scan} . It turns out the η values should somehow depends on scanning scheme. Again that's because when we determine the upper bound we treated \mathbf{r}_η as an arbitrary vector, such that we lose all information related to scanning scheme in the pointing matrix P .

Even though the perturbation parameter η get from Eq. (6) are not the most optimal, it still performs much

better than traditional conjugate gradient method under $1/f$ noise scenario without adding extra computational cost. The only extra free parameter added is to determine whether the error at current step $\mathbf{r}(\eta_i) = \|\mathbf{b}(\eta_i) - A(\eta_i)\mathbf{m}\|$ is small enough such that we advance to next value η_{i+1} .

Also this analysis of η value also explains why cooling parameters $\lambda = 1/\eta$ in messenger field are chosen to be geometric series or `logspace` used in Huffenberger & Naess (2018).

5. CONCLUSIONS

KMH: We need some discussion of the things that haven't yet been demonstrated with the PCG, like multiple messenger fields. Has the Kodi-Ramanah dual messenger field scheme been demonstrated in a PCG scheme by Papez?

All of the calculation are using simple preconditioner $P^\dagger P$, but the entire analysis is independent of preconditioner. Better preconditioners would also lead to improvements.

BQ and KH are supported by NSF award 1815887.

APPENDIX

A. THE SEQUENCE OF INVERSE COOLING PARAMETERS

We know that the initial inverse cooling parameter $\eta_0 = 0$. What would be good value for the next parameter η_1 ? To simplify notation, we use N_η to denote $N(\eta) = \tau I + \eta \bar{N}$. For some specific η value, the minimum χ^2 value is given by the optimized map $\hat{\mathbf{m}}(\eta) = (P^\dagger N_\eta^{-1} P)^{-1} P^\dagger N_\eta^{-1} \mathbf{d}$, which minimizes

$$\chi^2(\hat{\mathbf{m}}(\eta), \eta) = (\mathbf{d} - P\hat{\mathbf{m}}(\eta))^\dagger N_\eta^{-1} (\mathbf{d} - P\hat{\mathbf{m}}(\eta)). \quad (\text{A1})$$

We restrict to the case that the noise covariance matrix N is diagonal in the frequency domain, and represent the frequency-domain eigenvalues as N_f .

Let us first consider $\eta_1 = \eta_0 + \delta\eta = \delta\eta$ such that $\eta_1 = \delta\eta$ is very small quantity, $\delta\eta \ll 1$. Since $\hat{\mathbf{m}}(\eta)$ minimizes $\chi^2(\hat{\mathbf{m}}(\eta), \eta)$, we have $\frac{\partial}{\partial \hat{\mathbf{m}}} \chi^2(\hat{\mathbf{m}}(\eta), \eta) = 0$, and using chain rule

$$\frac{d}{d\eta} \chi^2(\hat{\mathbf{m}}(\eta), \eta) = \frac{\partial}{\partial \eta} \chi^2(\hat{\mathbf{m}}(\eta), \eta) = -(\mathbf{d} - P\hat{\mathbf{m}}(\eta))^\dagger N_\eta^{-1} \bar{N} N_\eta^{-1} (\mathbf{d} - P\hat{\mathbf{m}}(\eta)) \quad (\text{A2})$$

Then the fractional decrease of $\chi^2(\hat{\mathbf{m}}(0), 0)$ from $\eta_0 = 0$ to $\eta_1 = \delta\eta$ is

$$-\frac{\delta\chi^2(\hat{\mathbf{m}}(0), 0)}{\chi^2(\hat{\mathbf{m}}(0), 0)} = -\delta\eta \frac{\frac{d}{d\eta} \chi^2(\hat{\mathbf{m}}(0), 0)}{\chi^2(\hat{\mathbf{m}}(0), 0)} = \delta\eta \frac{1}{\tau} \frac{(\mathbf{d} - P\hat{\mathbf{m}}(0))^\dagger \bar{N} (\mathbf{d} - P\hat{\mathbf{m}}(0))}{(\mathbf{d} - P\hat{\mathbf{m}}(0))^\dagger (\mathbf{d} - P\hat{\mathbf{m}}(0))} \quad (\text{A3})$$

Here we put a minus sign in front of this expression such that it's non-negative, and use $N_{\eta=0} = \tau I$ at the second equality. Since it is hard to analyze $\mathbf{d} - P\hat{\mathbf{m}}$ under frequency domain, we treat it as an arbitrary vector, then the least upper bound is given by

$$-\frac{\delta\chi^2(\hat{\mathbf{m}}(0), 0)}{\chi^2(\hat{\mathbf{m}}(0), 0)} \leq \frac{\delta\eta}{\tau} \max(\bar{N}_f) \quad (\text{A4})$$

where $\max(\bar{N}_f)$ is the maximum eigenvalue of \bar{N} . Here if we assume that initial χ^2 value $\chi^2(\hat{\mathbf{m}}(0), 0)$ is much larger than final value $\chi^2(\hat{\mathbf{m}}(1), 1)$, $\chi^2(\hat{\mathbf{m}}(0), 0) \gg \chi^2(\hat{\mathbf{m}}(1), 1)$, then we would expect

$$-\frac{\delta\chi^2(\hat{\mathbf{m}}(0), 0)}{\chi^2(\hat{\mathbf{m}}(0), 0)} = 1 - \frac{\chi^2(\hat{\mathbf{m}}(1), 1)}{\chi^2(\hat{\mathbf{m}}(0), 0)} \approx 1 \quad (\text{A5})$$

The upper bound is strictly smaller than 1. Ideally, if $\delta\chi^2(\hat{\mathbf{m}}(0), 0) = \chi^2(\hat{\mathbf{m}}(1), 1) - \chi^2(\hat{\mathbf{m}}(0), 0)$, then it would get close to the final χ^2 at next iteration, but we do not know the final $\chi^2(\hat{\mathbf{m}}(1), 1)$. So we want $\left| \frac{\delta\chi^2(\hat{\mathbf{m}}(0), 0)}{\chi^2(\hat{\mathbf{m}}(0), 0)} \right|$ to be as large as possible, so it could converge fast, but subject to another constraint that the least upper bound cannot exceed 1. Therefore we can choose $\delta\eta$ such that the least upper bound is equal to 1. Thus we choose

$$\eta_1 \equiv \frac{\tau}{\max(\bar{N}_f)} = \frac{\min(N_f)}{\max(N_f) - \min(N_f)}. \quad (\text{A6})$$

Here N_f and \bar{N}_f are the eigenvalues of N and \bar{N} in the frequency domain. If the condition number of noise covariance matrix $\kappa(N) = \max(N_f)/\min(N_f) \gg 1$, then $\eta_1 \approx \kappa^{-1}(N)$.

What about the other parameters η_m with $m > 1$? We use a similar analysis, letting $\eta_{m+1} = \eta_m + \delta\eta_m$ with a small $\delta\eta_m \ll 1$, and set the least upper bound of relative decrease equal to 1.

$$\begin{aligned} -\frac{\delta\chi^2(\hat{\mathbf{m}}(\eta_m), \eta_m)}{\chi^2(\hat{\mathbf{m}}(\eta_m), \eta_m)} &= \delta\eta_m \frac{(\mathbf{d} - P\hat{\mathbf{m}}(\eta_m))^\dagger N_{\eta_m}^{-1} \bar{N} N_{\eta_m}^{-1} (\mathbf{d} - P\hat{\mathbf{m}}(\eta_m))}{(\mathbf{d} - P\hat{\mathbf{m}}(\eta_m))^\dagger N_{\eta_m}^{-1} (\mathbf{d} - P\hat{\mathbf{m}}(\eta_m))} \\ &\leq \delta\eta_m \max \left(\frac{\bar{N}_f}{\tau + \eta_m \bar{N}_f} \right) \end{aligned} \quad (\text{A7})$$

The upper bound in the second line is a little bit tricky. Both matrix \bar{N} and $N_{\eta_m}^{-1}$ can be simultaneously diagonalized in frequency space. For each eigenvector \mathbf{e}_f , the corresponding eigenvalue of the matrix on the numerator $N_{\eta_m}^{-1} \bar{N} N_{\eta_m}^{-1}$ is $\lambda_f = \bar{N}_f (\tau + \eta_m \bar{N}_f)^{-2}$, and the eigenvalue for matrix on the denominator $N_{\eta_m}^{-1}$ is $\gamma_f = (\tau + \eta_m \bar{N}_f)^{-1}$. Their eigenvalues are related by $\lambda_f = [\bar{N}_f / (\tau + \eta_m \bar{N}_f)] \gamma_f$. For any vector $\mathbf{v} = \sum_f \alpha_f \mathbf{e}_f$, we have

$$\frac{\mathbf{v}^\dagger N_{\eta_m}^{-1} \bar{N} N_{\eta_m}^{-1} \mathbf{v}}{\mathbf{v}^\dagger N_{\eta_m}^{-1} \mathbf{v}} = \frac{\sum_f \alpha_f^2 \lambda_f}{\sum_f \alpha_f^2 \gamma_f} = \frac{\sum_f \alpha_f^2 \gamma_f \bar{N}_f / (\tau + \eta_m \bar{N}_f)}{\sum_f \alpha_f^2 \gamma_f} \leq \max \left(\frac{\bar{N}_f}{\tau + \eta_m \bar{N}_f} \right). \quad (\text{A8})$$

Similarly, we could set the least upper bound equal to 1. Then we get

$$\delta\eta_m = \min \left(\frac{\tau + \eta_m \bar{N}_f}{\bar{N}_f} \right) = \eta_m + \frac{\tau}{\max(\bar{N}_f)}. \quad (\text{A9})$$

Therefore

$$\eta_{m+1} = \eta_m + \delta\eta_m = 2\eta_m + \frac{\tau}{\max(\bar{N}_f)} \quad (\text{A10})$$

The final term $\tau/\max(\bar{N}_f) = \eta_1$ becomes subdominant after a few terms, and we see that the η_m increase like a geometric series. Here we assumed that $\chi^2(\hat{\mathbf{m}}(\eta_m), \eta_m) \gg \chi^2(\hat{\mathbf{m}}(1), 1)$, which we expect it to be satisfied for our assumed $\eta_m \ll 1$. Since the final result is geometric series, only the last few η_m values fail to be much smaller than 1. If written in the form $\eta_{m+1} + \tau/\max(\bar{N}_f) = 2(\eta_m + \tau/\max(\bar{N}_f))$ it's easy to see that for $m \geq 1$, $\eta_m + \tau/\max(\bar{N}_f)$ forms a geometric series

$$\eta_m + \frac{\tau}{\max(\bar{N}_f)} = \left(\eta_1 + \frac{\tau}{\max(\bar{N}_f)} \right) 2^{m-1} = \frac{\tau}{\max(\bar{N}_f)} 2^m \quad (\text{A11})$$

where we used $\eta_1 = \tau/\max(\bar{N}_f)$. Note that $m = 0$ and $\eta_0 = 0$ also satisfy this expression and we've got final expression for all η_m

$$\eta_m = \min \left\{ 1, \frac{\tau}{\max(\bar{N}_f)} (2^m - 1) \right\} \quad (\text{A12})$$

Here we need to truncate the series when $\eta_m > 1$.

REFERENCES

- | | |
|--|--|
| <p>482 Dünner, R., Hasselfield, M., Marriage, T. A., et al. 2013,
 483 ApJ, 762, 10, doi: 10.1088/0004-637X/762/1/10</p> <p>484 Elsner, F., & Wandelt, B. D. 2013, A&A, 549, A111,
 485 doi: 10.1051/0004-6361/201220586</p> <p>486 Haffenberger, K. M., & Næss, S. K. 2018, The
 487 Astrophysical Journal, 852, 92,
 488 doi: 10.3847/1538-4357/aa9c7d</p> | <p>489 Janssen, M. A., & Gulkis, S. 1992, in NATO Advanced
 490 Science Institutes (ASI) Series C, ed. M. Signore &
 491 C. Dupraz, Vol. 359 (Springer), 391–408</p> <p>492 Kodi Ramanah, D., Lavaux, G., & Wandelt, B. D. 2017,
 493 MNRAS, 468, 1782, doi: 10.1093/mnras/stx527</p> <p>494 Papež, J., Grigori, L., & Stompor, R. 2018, A&A, 620, A59,
 495 doi: 10.1051/0004-6361/201832987</p> <p>496 Tegmark, M. 1997, ApJL, 480, L87, doi: 10.1086/310631</p> |
|--|--|